Analysis of start energy of Stirling engine type alpha

JACEK KROPIWNICKI[*]

Gdańsk University of Technology Faculty of Mechanical Engineering,
Narutowicza 11/12, 80-233 Gdańsk, Poland

Abstract   The Stirling engine type alpha is composed of two cylinders (expansion space E and compression space C), regenerator that forms the space between the cylinders and the buffer space (under the pistons). Before the start-up and as a result of long-term operation, the average pressure in the working space (above the pistons) and in the buffer space is the same. However, in the initial phase of operation, the average pressure in the working space is different then the average pressure in the buffer space depending on the crankshaft starting position (starting angle). This, in turn, causes a large variation in the starting torque. An additional unfavorable factor caused by a large variation in the course of the indicated torque is the rotational speed variation and the formation of torsional vibrations in the drive system. After some time, depending on the quality of the engine piston sealing, the average pressure in the working and buffer space will equalize. The occurrence of the above-described phenomenon affects the selection of the starting electric motor, which can be significantly reduced, when the crankshaft starting position is optimized (the starting torque is several times greater than the average torque occurring in the generator operation mode). This paper presents the analysis of the impact of the crankshaft starting position on the course of the indicated torque and the resulting start-up energy. Starting the engine at an unfavorable position of the crankshaft may, in extreme cases, increase the starting torque even three times.

Keywords: Stirling engines; System efficiency; Low temperature supply

---

[*]Email: jkropiwn@pg.gda.pl

1 Introduction

The Stirling engine (SE) is a thermal engine that converts thermal energy into mechanical energy, but without the internal combustion process [1,2], and as a result of supplying heat from outside. The source of heat can be the process of burning fuel in the combustion chamber, waste energy from another heat device, heat from geothermal sources or solar energy. Stirling engines can be supplied with thermal energy derived from the combustion of any fuel, e.g., natural gas, biogas, gasoline, heating oil, vegetable oil and biomass [3,4]. The current increase in interest in Stirling engines is related mainly to striving for better use of low-calorie and low-energy sources but also for solar energy. Stirling engines are characterized by a relatively simple construction in comparison to internal combustion engines [5,6], moving parts of the engine do not have direct contact with the substance supplying thermal energy to the device and they operate at lower temperature differences [7]. All this affects the durability of Stirling engines, and often eliminates service at all. The Stirling engine, in combination with the power generator is also used as a reliable source of electricity with relatively high efficiency [8,9,28,29], also achieved at very low power devices. Currently, as a result of the worldwide growing interest in the use of renewable energy sources to generate electricity, it is conducted a series of research on Stirling engines [10–13].

Cheng *et al.* [14] developed and tested a beta type Stirling engine with a rhombic-drive mechanism (displacer diameter: 0.07 m, displacer swept volume: 0.000135 m^3). The experiments were conducted for two different working gases (air and helium) and at various charged pressures and heating temperatures. For helium, as the working gas, at a charged pressure of 800 kPa and heating temperature of 850 °C, the shaft power of the engine can reach 390 W at 1400 rpm with 1.21-kW input heat transfer rate (32.2% thermal efficiency). For air as the working gas at a charged pressure of 600 kPa and a heating temperature of 650 °C, the shaft power of the engine can reach 60 W at 700 rpm. Gheith *et al.* [15] tested a gamma type Stirling engine with air as the working gas (displacer diameter 0.095 m, displacer swept volume: 0.00085 m^3). The maximum brake power of 355 W was obtained for a charging pressure of 800 kPa and a heating temperature of 500 °C at 600 rpm. Due to the accomplished tests and calculations for the heating temperature of 300 °C the expected brake power is 150 W. Karabulut *et al.* [16] designed and manufactured a beta type Stirling engine (displacer diameter: 0.069 m, displacer swept volume: 0.000295 m^3), which

works at relatively lower temperatures. The experimental results presented by researchers were obtained by testing the engine with air as working gas. The hot end of the displacer cylinder was heated with a liquefied petroleum gas (LPG) flame and kept atabout $200\,^\circ$C. The maximum power output was obtained at 280 kPa with the charge pressure equal to 52 W at 453 rpm. The thermal efficiency corresponding to the maximum power was determined as 15%. Kongtragool *et al.* [17] designed and constructed four power pistons, gamma type, low temperature, differential Stirling engine (displacer diameter: 0.032 m, displacer swept volume: 0.006394 m^3). The engine performance was tested with air at an atmospheric pressure by using a gas burner as a heat source and a heating temperature of $498\,^\circ$C. The engine produces the maximum shaft power of 32.7 W at 42.1 rpm and a maximum brake thermal efficiency of 0.81%. Li *et al.* [18] developed a beta type Stirling engine with an output shaft power of several kilowatts, which could be driven by mid-high temperature waste gases (displacer diameter: 0.102 mm, displacer swept volume: 0.000462 m^3). The engine performance was tested with helium at a charged pressure of 2000 kPa and a heating temperature of approx. $500\,^\circ$C. The maximum power output was obtained as 3476 W at 1248 rpm. The thermal efficiency corresponding to maximum power was determined as 26%. Sripakagorn *et al.* [19] developed a beta-type Stirling engine (displacer diameter: 0.074 m, displacer swept volume: 0.000165 m^3). The engine performance was tested with air as the working gas at a charged pressure of 700 kPa and a heating temperature of $500\,^\circ$C. The shaft power of the engine can reach 95 W at 360 rpm (9.35% thermal efficiency). Under the atmospheric pressure, the engine produces a maximum power of 3.8 W at 205 rpm and $350\,^\circ$C. A free piston (beta type) Stirling engine was invented by Lane and Beale [12] (displacer diameter: 0.044 m, displacer stroke: 0.04 m). The stable engine operation was obtained at the temperature range of 120–$150\,^\circ$C at the heater section (initial gas pressure: 101 kPa). The maximum efficiency of 5.6% at 6.4 Hz of frequency was obtained.

A prototype of the Stirling alpha engine (diameter/stroke: 0.13 m/0.055 m) was developed in the laboratory of the Faculty of Mechanical Engineering of the Gdańsk University of Technology (Fig. 1). The engine can be driven by mid-high temperature waste gases coming from an internal combustion engine (Fig. 2). The engine performance was tested with air as the working gas at a charged pressure of 200–500 kPa and a heating temperature of 200–$400\,^\circ$C.
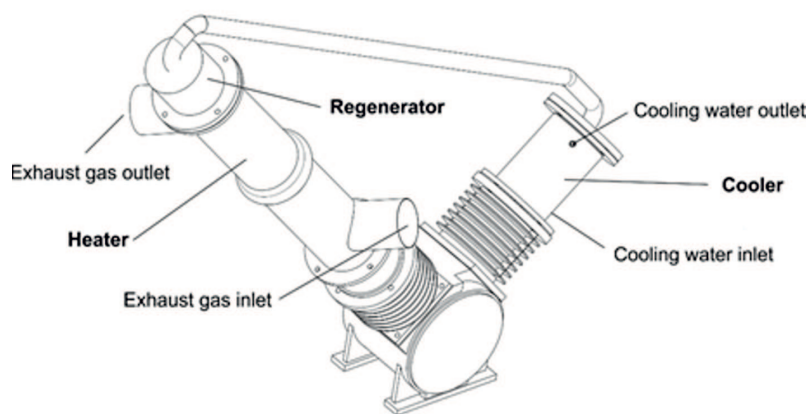
Figure 1: Scheme of the prototype Stirling alpha engine.

The tests were carried out at a rotational speed of 200 rpm using an external drive. During the tests, it turned out that the power of the mechanical and hydraulic resistance of the device exceeds the power indicated in the Stirling engine and the engine is not able to work independently. The results presented in Fig. 3 show that the indicated work for the supply temperature is 210 °C and the average pressure of the 230 kPa is 2.3 J and successively increases with the increase of temperature and pressure up to 13 J. It was estimated that for a pressure of 460 kPa the sum of hydraulic and mechanical losses is 17 J. To start the engine, it is necessary to increase the indicated work or significantly reduce the losses.

Commercially available on market Stirling engines are usually sold as combined heat and power units fueled by natural gas or diesel fuel. An example of a cogeneration unit, which can be supplied with energy from renewable sources, is the unit from Stirling DK [25]. The system consists of an expanded combustion chamber, four-cylinders, a two-sided alpha type Stirling engine and an electric generator enclosed in a sealed housing. This arrangement enables the engine to be supplied with the thermal energy derived from burning wood waste in the form of chips. The operational electrical efficiency of 28% is achieved at a power output 30 kWe. For the correct operation of the device the burning gas temperature, in the combustion chamber, should not be lower than 1000 °C.

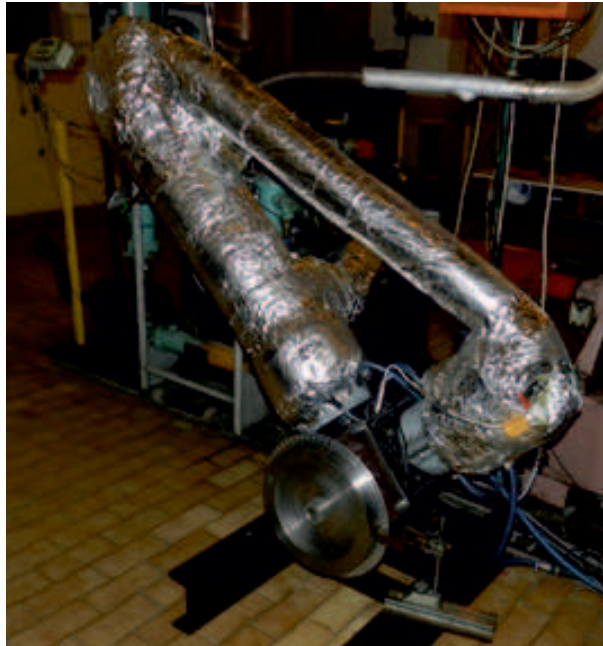Another example of a commercial cogeneration unit with the Stirling

Figure 2: System powered by exhaust gases from a spark-ignition engine.

engine, which can be supplied with energy from renewable sources, is the unit from Stirling Biopower [26]. This arrangement also consists of a four cylinder, two-sided alpha type Stirling engine and an electric generator enclosed in a sealed housing. The combustion of biomass takes place in a separate unit that heats air supplied to the heater. For the correct operation of the device the temperature of air supplied to the heater should not be lower than 500 °C. The system is also equipped with an integrated combustion chamber, which supplies flue gases to the heater. The integrated chamber can be supplied with the following gases: Compressed Natural (CNG), liquefied petroleum gas (LPG), biogas, and synthetic gas, and hydrogen. Operating with gaseous fuels of energy densities 13 MJ/Nm^3 and higher the electrical efficiency of 29% at 38 kWe can be achieved.

In the above described research works designed engines are pretending to be powered by waste or renewable energy of relatively low temperature (below 350 °C), which stays in contrast to the operating conditions common for commercialized Stirling engines powered by high temperature sources (usually above 1000 °C). This assumption causes a few restrictions, which
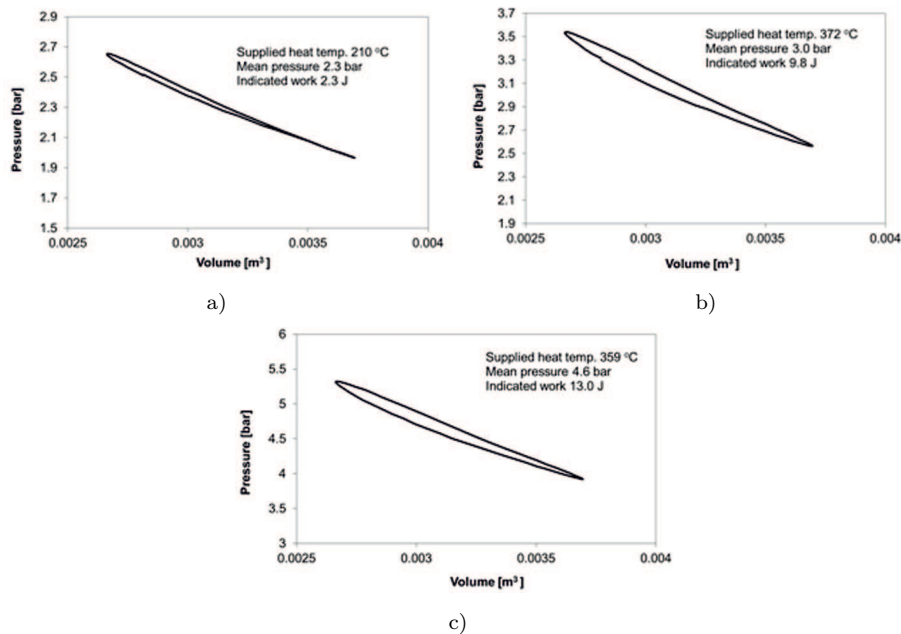
Figure 3: Pressure – volume diagrams of the tested alpha type Stirling engine for the mean pressure of the working gas: a) 230 kPa, b) 300 kPa, c) 460 kPa.

have been pointed out below:

- Due to the low density of the thermal energy applied to the engine, the indicated power is also of low density and can be easily entirely consumed by internal mechanical and hydraulic resistance. Therefore, it is expected that mechanical and hydraulic resistance will be significantly reduced compared to high temperature devices. Low pressure working gas (up to 2000 kPa) is commonly used by researchers.

- An increase of heat exchange surface of the heater is expected as well as intensification of the heat exchange process itself to increase the indicated power. The above solution causes an increase in the dead volume, which contributes to the reduction of the thermal efficiency of the device.

- Due to the expected low friction coming from the sealing, increased leakages are expected and accepted. Therefore, air is preferred as a working gas – easy to compensate the leakages.

- Due to the risk of oil self-ignition (compressed air in the device), the non-oil bearings are preferred.

- Due to the reduced power density of the device, the electric generator can be reduced. Unfortunately, the same electric machine is used to produce electricity and to start the Stirling engine. It is recommended to limit the start-up energy of the Stirling engine so that the size of the electric machine depends on the generator work not the propulsive one.

In this work, the analysis of the last restriction implementation has been performed. Calculations of the start-up phase of the Stirling type alpha engine were carried out, determining the maximum drive torque needed to perform the first compression cycle.

2 The analysis of the start-up energy

The Stirling engine type alpha (Fig. 4) is composed of two cylinders (expansion space E and compression space C), the regenerator that forms the space between the cylinders and the buffer space (under the pistons) [7]. Heat from the energy source, e.g., in the form of a low temperature flue gas stream, is supplied to the expansion space *via* heat exchangers [20–22], whereas from the compression space heat is removed at a lower temperature than the heat supplied to the expansion space. In the working space and in the buffer space there is a working gas, most often helium, hydrogen, nitrogen or air. In commercial solutions, usually the engine is sealed and there is no need to refill any leakage of the working gas [23]. In contrast, the working space is separated from the buffer space by means of movable seals, usually piston rings, which do not ensure full tightness. Before the start-up and as a result of long-term operation, the average pressure in the working space (above the pistons) and in the buffer space is the same. However, in the initial phase of operation, the average pressure in the working space is different to the pressure in the buffer space depending on the crankshaft starting position (starting angle).

A calculation has been made using the isothermal Schmidt model [1,2]. The analysis has been proceeded for the assumed constant temperature of working gas in the expansion space (heater) and in the compression space (cooler). The case analyzed below concerns the engine start-up (mainly the first crankshaft revolution), when the temperatures of the working gas
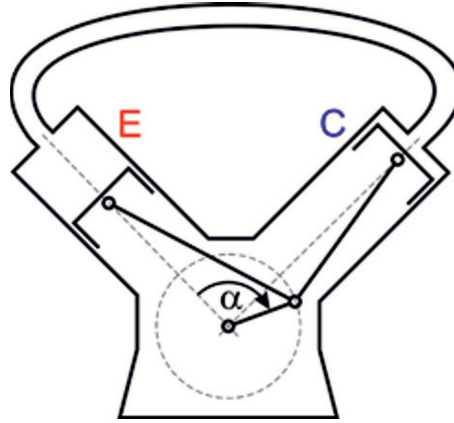
Figure 4: Layout of the analyzed Stirling engine: E – expansion space, C – compression
          space.

and exchanger walls are leveled. The first revolution cycle itself has a much
slower speed than the subsequent work cycles for the determined heat sup-
plied and discharged from the engine, which prompts to describe the phe-
nomenon rather as an isothermal than as an adiabatic model case. In Tab. 1
basic specification of the analyzed Stirling engine has been shown.

An important factor that can influence the pressure course in the work-

Table 1: The main parameters and proprieties of the analyzed alfa type Stirling engine.

Parameter	Value
Rotational speed	750 rpm
Working gas	air
Charge pressure	1000 kPa
Compression (cold) volume: diameter/ stroke	0.13 m/0,055 m
Compression (cold) volume: swept volume	0.00073 m^3
Expansion (hot) volume: diameter/ stroke	0.13 m/0.055 m
Expansion (hot) volume: swept volume	0.00073 m^3
Temperature of working gas in the cold volume	60 °C
Temperature of working gas in the hot volume	200 °C
Mechanical and pumping losses in the engine	250 W

ing space may be the gas leakage taking place between the cylinders and the buffer space through the piston sealing rings. In order to determine the effect of this phenomenon on the parameters of the working gas, calculations were made of the gas leakage ($\dot{m}_{leak}$) from the working space to the buffer (symbol +) and in the opposite direction (symbol –) [24]:

$$\dot{m}_{leak} = \pi D \left(\frac{\triangle p h^3}{12 \mu l} + \frac{wh}{2} \right) \ , \tag{1}$$

where: D – the diameter of the cylinder, Dp – the pressure drop on the first piston ring, h – the mean height of the gap, m – the dynamic viscosity of the gas, l – the length of the piston, w – the speed of the piston.

During the calculations it was assumed that the mean height of the gap is the same for the expansion and compression cylinders and equals 6×10^{-6} m. Due to the analyzed range of the operation of the engine, the calculations have been performed for the designed engine speed 750 rpm, as well as 50% and 10% of the target speed. In particular the lowest speed should be best suited to the first revolution of the crankshaft. In the calculations, initially implemented the isothermal Schmidt model has been used for the determination of pressure and temperature of the working gas, the analyzed case concerns the recognized most unfavorable crankshaft starting position, which maintaining some mean pressure difference between the working space and the buffer space (a detailed description of the phenomenon has been put in the next part of the section). In Fig. 5 the results of calculations have been presented. It can be observed that the lifting effect associated with the piston movement (the component with the speed of the piston in Eq. (1)) has a stronger damping impact on the gas leakage for the compression cylinder. According to Eq. (1) the increase of the rotational speed, for the assumed same pressure drop, causes the increase of leakage due to intensification of the lifting effect. This regularity can be clearly observed by analyzing the gas leakage for the tested rotational speed of the crankshaft (Fig. 6). In turn, the increase of rotational speed causes a decrease of the one cycle period and, as a result, a reduction of the total mass of the gas leaking into the buffer space in relation to the mass of the gas closed in the working space. In Fig. 7 the gas leakage share (in relation to the mass in the working space) for the one crankshaft revolution has been presented.
The largest gas leakage share was observed at the rotational speed of 10% of the target speed, for the crankshaft position interval between 36 and 72 deg
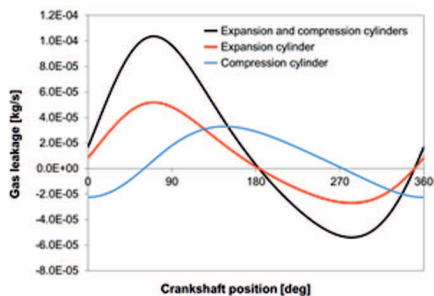
Figure 5: Gas leakage from the working space to the buffer (symbol +) and in the opposite direction (symbol -) at 750 rpm.
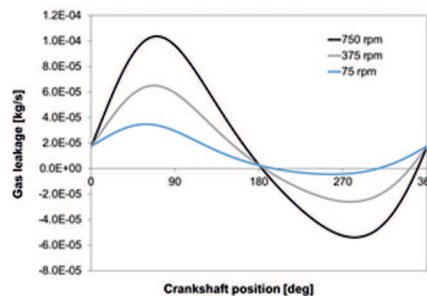
Figure 6: Gas leakage comparison for the crankshaft speed 750, 375, and 75 rpm.

and it is approx. 0.01%. In the case of the full revolution of the crankshaft, the gas leakage share is at 750, 375, and 75 rpm, respectively: 5.27×10^{-5}, 8.84×10^{-5}, and 3.74×10^{-4} kg/s. Analyzing the initial phase of the engine start-up, it can be assumed that the gas leakage does not constitute a significant influence on the pressure course in the engine working space and can be omitted in further calculations.
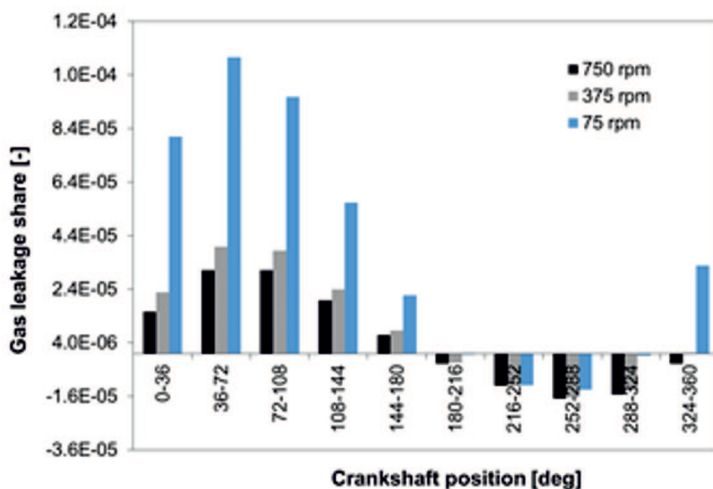

Figure 7: Gas leakage share (in relation to the mass in the working space) for one crankshaft revolution.

The starting position of the crankshaft determines the mass of the working gas closed in the working space (Fig. 8). The rotation of the crankshaft causes changes in the volume of the working space, which in combination with the processes of supplying or removing heat from the working gas, causes cyclic pressure changes (Fig. 9). The considered variation of pressure in the working space causes in turn a variable indicated torque, the extreme values of which are related to the compression (maximum) and expansion (minimum). Both the compression and the expansion process requires firstly consuming a large amount of energy (taken from the flywheel) and then accumulating its overproduction. As a result the more energy is needed to be accumulated during expansion or spent during compression, the larger the flywheel must be used to avoid large changes in engine speed or in the extreme situation stopping the engine in the compression process. Energy which must be collected in the flywheel during temporary acceleration (expansion) or generated during temporary deceleration (compression) can be calculated basing on the course of the indicated torque

$$E = \int_{\alpha_0}^{\alpha_1} |T_{ind} - T_{av}| d\alpha \ , \tag{2}$$

where: E – energy, which must be collected in the flywheel, T_{ind} – indicated torque, T_{av} – average value of the indicated torque (over the cycle), a_0 – position of the crankshaft for the start of the energy collection, a_1 – position of the crankshaft for the end of the energy collection.

Having assumed the permissible angular velocity range of the system the expected flywheel the moment of inertia can be calculated using the following formula:

$$E = \frac{1}{2}\Big(I_{eng} - I_{fly}\Big)\left(\omega_{max}^2 - \omega_{mihn}^2\right) \ , \tag{3}$$

where: I_{eng} – engine moment of inertia, I_{fly} – flywheel moment of inertia, ω_{min} – minimum crankshaft angular velocity, ω_{max} – maximum crankshaft angular velocity.

Assuming that the average angular velocity of the system is known

$$\omega_{av} = \frac{\omega_{max} + \omega_{min}}{2} \tag{4}$$

and permissible angular velocity range is described by the degree of velocity variation

$$\delta = \frac{\omega_{max} - \omega_{min}}{\omega_{av}} \ , \tag{5}$$

where d is the degree of velocity variation (over the cycle), for the electric generators usually $1/200$, and ω_{av} is the average crankshaft angular velocity, Eq. (3) can be simplified to the following form:

$$I_{fly} = \frac{E}{\delta\omega_{av}^2} - I_{eng} \, . \tag{6}$$

It can be noticed that the energy, which must be accumulated, corresponds directly to the moment of inertia, and thus the size of the entire engine.
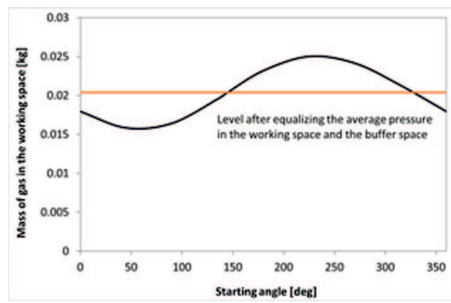

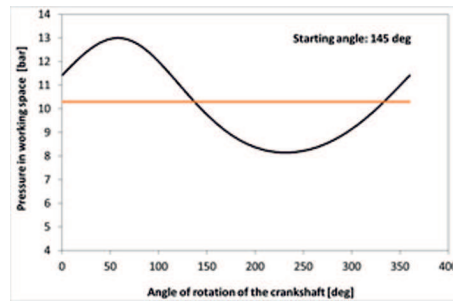Figure 8: The effect of starting angle on the mass of working gas.

Figure 9: Pressure in working space for the long-term operation or for the starting angle 145 deg.

In Figs. 10–13 the results of calculations have been presented for the following starting angle: 0, 90, 145, and 270 deg. In Fig. 10 it can be noticed that the amplitude of the indicated torque is about 10 times greater than the mean value. The compression as well as the expansion process takes a relatively long time. The situation is even worse for the starting angle 90 deg (Fig. 11). There are still four changes in the direction of the indicated torque but the processes of compression and expansion are longer and of a higher amplitude.

For 145 deg (Fig. 12), the situation is very similar to that one of 0 deg but the compression process requires significantly less energy, also the amplitude in the compression is much smaller That potentially means a smaller electrical machine for the start-up process (a smaller locked rotor torque). As it was previously pointed out, the situation showed in Fig. 12 corresponds to the long term operation. Due to the leakages caused by the movable seals, placed between the working and buffer space (on pistons), the average pressure in the working space (above the pistons) and in the buffer
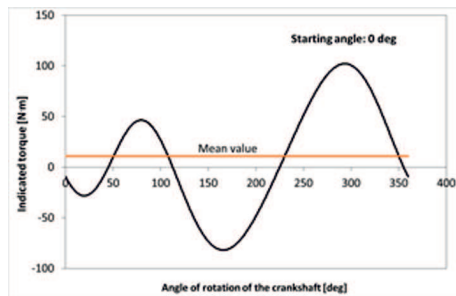
Figure 10: The indicated torque for the starting angle 0 deg.
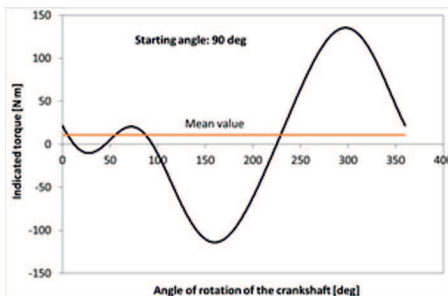

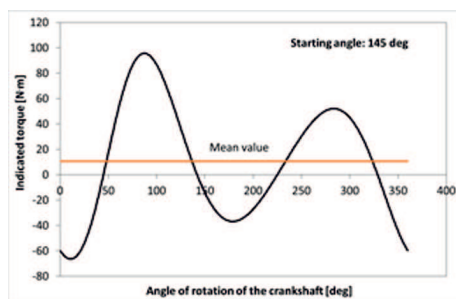Figure 11: The indicated torque for the starting angle 90 deg.

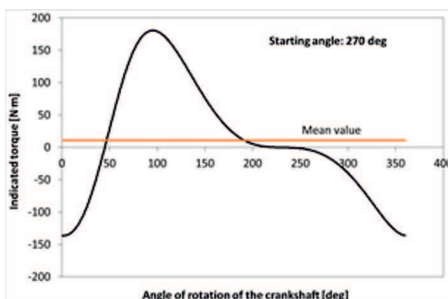Figure 12: The indicated torque for the starting angle 145 deg.

Figure 13: The indicated torque for the starting angle 270 deg.

space will equalize. The calculation carried out by the iteration process allowed to determine the starting angle, for which the average pressure is the same on both sides. The last analyzed starting angle (Fig. 13) concerns a very unfavorable situation, when the direction of the indicated torque changes only two times per cycle, the process of compression is very energy consuming and the amplitude of this process is extremely high. Using relation (2) the energy, which must be collected in the flywheel has been calculated for the starting angle 145 and 270 deg and it is respectively 72 and 230 J. This means that the energy needed to be accumulated for the next compression in the flywheel for the 270 deg starting angle is almost 4 times bigger than the possible minimum (145 deg), the moment of inertia of the flywheel calculated using Eq. (6) would also be 4 times bigger.

In Fig. 14 a summary of the influence of the starting angle on the

amplitude of the indicated torque in the compression process has been pre-
sented. It can be observed that the most favorable situation takes place for
the starting angle 145 deg, which corresponds to the long term operation.
The worst situation takes place for 230 deg. The amplitude of the indicated
torque in the compression process is even three times bigger than in the
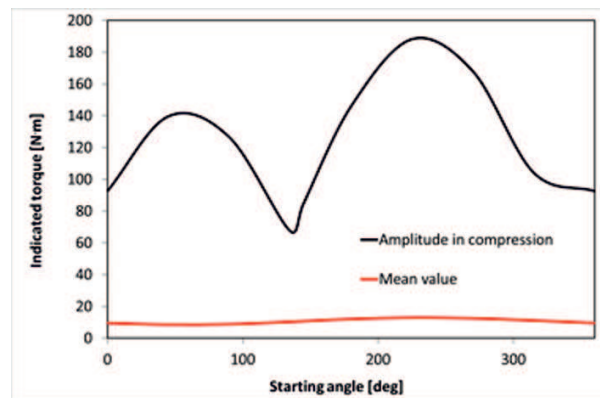most favorable situation.

Figure 14: The amplitude of the indicated torque in the compression process *vs.* the
starting angle.

3   Conclusions

The torque sequence during the motor start-up is strongly dependent on
the starting position of the crankshaft (the starting angle). This, in turn,
causes a large variation in the indicated torque. An additional unfavorable
factor caused by a large variation in the course of the indicated torque is the
rotational speed variation and the formation of the torsional vibrations in
the drive system. After some time, depending on the quality of the engine
piston sealing, the average pressure in the working and the buffer space
will equalize and the observed large variation in the indicated torque will
be neutralized (suppressed). Anyway, the occurrence of this phenomenon
has a huge impact on the start-up phase and determines the size of the
electric machine used for the start of the engine.

     The paper presents the analysis of the impact of the crankshaft starting
position (the starting angle) on the course of the indicated torque. The
analysis has been performed for the assumed constant temperature of the

working gas in the expansion space (heater) and in the compression space (cooler). Based on the obtained results it can be noticed that the amplitude of the indicated torque can be up to 20 times bigger than the mean value. Both the compression and the expansion processes can take a relatively long time and require firstly consuming a large amount of energy, taken from the flywheel, and then accumulating its overproduction. As a result the more energy is needed to be accumulated during expansion or spent during compression, the larger the flywheel must be used to avoid large changes in engine speed or in the extreme situation stopping the engine in the compression process. Presented in Fig. 14 a summary of the influence of the starting angle on the amplitude of the indicated torque in the compression process shows that the most favorable situation takes place for the starting angle 145 deg, which corresponds to the long term operation. The worst situation takes place for 230 deg. The amplitude of the indicated torque in the compression process is even three times bigger than in the most favorable situation.

A solution to the above described problem of engine start-up with an incorrect starting angle can be solved in two ways. The angle of the crankshaft position at which the engine is started or when the working and buffer spaces are separated can to be controlled by mechatronic elements. An additional advantage of this solution is the possibility of continuous power regulation. The second way is stopping the engine in a dedicated crankshaft position – a solution successfully applied in internal combustion engines with the 'Start&Stop' system produced by Mazda [27]

References

[1] WALKER G.: *Stirling Engines.* Oxford University Press, 1980.

[2] ŻMUDZKI S.: Stirling Engines. WNT, Warszawa 1993 (in Polish).

[3] FINKELSTEIN TH., ORGAN A.J.: *Air Engines.* ASME, New York 2001.

[4] BUORO D. ET AL.: *Optimal synthesis and operation of advanced energy supply systems for standard and domotic home.* Energ. Convers. Manage. **60**(2012), 96–105.

[5] BERND TH.: *Benchmark testing of micro-CHP units.* Appl. Therm. Eng. **28**(2008) 2049–2054.

[6] HARRISON J.: *Micro Combined Heat & Power.* EA Technology SYNOPSIS, 2002.

[7] KROPIWNICKI J.: *Design and applications of modern Stirling engines.* Combust. Eng. **3**(2013), 243–249.

[8] Cieśliński J., Kropiwnicki J., Kneba Z.: *Application of Stirling engines in micro-co-generation.* In: District Heating, Heating, Renewable Energy Ssources (W. Zima, D. Taler), Wydaw. Politechniki Krakowskiej, Kraków 2013, 49–60 (in Polish).

[9] Cieśliński J., Kropiwnicki J., Kneba Z., Woronkin S., Witanowski Ł., Zalewski K.: *Investigation of a Stirling engine as a micro-CHP system.* In: Proc. 3rd Int. Conf. Low Temperature and Waste Heat Use in Energy Supply Systems Theory and Practice, Bremen 2012, 33–38.

[10] Kropiwnicki J.: *Stirling engines powered by renewable energy sources.* In: Proc. 22nd Int. Sym. Research-Education-Technology, Bremen 2015, 231–237.

[11] Gianluca V. et al.: *Experimental and numerical study of a micro-cogeneration Stirling engine for residential applications.* Energy Procedia **45**(2014), 1235–1244.

[12] Lane N.W., Beale W.T.: *A Biomass-fired 1 kWe Stirling engine generator and its applications in South Africa.* In: Proc. 9th Int. Stirling Engine Conf., South Africa, June 2–4, 1999.

[13] Maier Ch., et al.: *Stirling Engine.* University of Gävle, Gävle 2007.

[14] Cheng C.H. et al.: *Theoretical and experimental study of a 300-W beta-type Stirling engine.* Energy **59**(2013), 590–599.

[15] Gheith R., Aloui F., Ben Nasrallah S.: *Experimental investigation of a Gamma Stirling engine.* Int. J. Energ. Res. **37**(2013), 1519–1528.

[16] Karabulut H., et al.: *An experimental study on the development of a b-type Stirling engine for low and moderate temperature heat sources.* Appl. Energ. **86**(2009), 68–73.

[17] Kongtragool B., Wongwises S.: *Performance of low-temperature differential Stirling engines.* Renew. Energ. **32**(2007), 547–566.

[18] Li T., et al.: *Development and test of a Stirling engine driven by waste gases for the micro-CHP system.* Appl. Therm. Eng. **33-34**(2012), 119–123.

[19] Sripakagorn A., Srikam C.: *Design and performance of a moderate temperature difference Stirling engine.* Renew. Energ. **36**(2011), 1728–1733.

[20] Mou J, Hong G.: *Startup mechanism and power distribution of free piston Stirling engine.* Energy **123**(2017), 655–663.

[21] Tavakolpour-Saleh A.R., et al.: *A novel active free piston Stirling engine: Modeling, development, and experiment.* Appl. Energ. **199**(2017), 400–415.

[22] Kwankaomeng S., et al.: *Investigation on stability and performance of a free-piston Stirling engine.* Energy Procedia **52**(2014), 598–609.

[23] Remiorz L., et al.: *Comparative assessment of the effectiveness of a free-piston Stirling engine-based micro-cogeneration unit and a heat pump.* Energy **148**(2018), 134–147.

[24] Jasiński R.: *Operating of components of hydraulic drive of machines in low ambient temperatures.* Wydaw. Politechniki Gdańskiej, Gdańsk 2018.

[25] Stirling DK, http://www.stirling-energie.de (accessed: June 30th 2019).

[26] Stirling Biopower, http://www.biowkk.eu/wp-content/uploads/2015/02/12748858113-Qalovis-Shrieves-Flexgen.pdf(accessed: June 30th 2019).

[27] Mazda, https://www2.mazda.com/en/csr/environment/special_ features/2009_ 02_ 01.html (accessed: June 30th 2019).

[28] UCHMAN W., REMIORZ L., KOTOWICZ J.: *Economic effectiveness evaluation of the free piston Stirling engine-based micro-combined heat and power unit in relation to classical systems.* Arch. Thermodyn. **40**(2019), 1, 71–83.

[29] RANJAN R.K., VERMA S.K.: *Thermodynamic analysis and analytical simulation of the Rallis modified Stirling cycle.* Arch. Thermodyn. **40**(2019), 2, 35–67.